

# The Phase Stability Network of All Inorganic Materials

Vinay I. Hegde,<sup>1,\*</sup> Muratahan Aykol,<sup>2,\*‡</sup> Scott Kirklin,<sup>1,†</sup> and Chris Wolverton<sup>1,‡</sup>

<sup>1</sup>*Department of Materials Science and Engineering,*

*Northwestern University, Evanston, IL 60208*

<sup>2</sup>*Toyota Research Institute, Los Altos, CA 94022*

arXiv:1808.10869v2 [cond-mat.mtrl-sci] 5 Nov 2022

---

\*These authors contributed equally to this work

†Current address: Jump Trading LLC, Chicago, IL 60654

‡Email: [c-wolverton@northwestern.edu](mailto:c-wolverton@northwestern.edu) (C. Wolverton), [murat.aykol@global.tri](mailto:murat.aykol@global.tri) (M. Aykol)

One of the holy grails of materials science, unlocking structure-property relationships, has largely been pursued via bottom-up investigations of how the arrangement of atoms and interatomic bonding in a material determine its macroscopic behavior. Here we consider a complementary approach, a top-down study of the organizational structure of networks of materials, based on the interaction between materials themselves. We unravel the complete “phase stability network of all inorganic materials” as a densely-connected complex network of 21,000 thermodynamically stable compounds (nodes) interlinked by 41 million tie-lines (edges) defining their two-phase equilibria, as computed by high-throughput density functional theory. We find that the node connectivity in the materials network has a lognormal distribution, and the connectivity decreases with the number of elemental constituents in a material. Analyzing the topology of this network of materials has the potential to uncover new knowledge inaccessible from traditional atoms-to-materials paradigms. Using the connectivity of nodes in the phase stability network, we derive a rational, data-driven metric for material reactivity, the “nobility index”, and quantitatively identify the noblest materials in nature.

## Introduction

Several diverse complex systems are modeled as networks of discrete components linked together: man-made systems such as electrical power grids and the world-wide web (1, 2), social systems such as friendship and scientific collaborations (3, 4), and natural systems such as metabolism in a cell and food-webs (5, 6). Despite significant variation in the nature of individual components and interconnections, many of these networks show striking similarities in their topology (7, 8), often providing new insights into each respective domain of knowledge. For instance, disparate systems such as the world-wide web and metabolic reactions in cellular organisms both have been shown to follow the organizational principles of robust, error-tolerant scale-free networks, with implications for the resilience of the internet and the design of therapeutics (8, 9), respectively.

Recent developments in high-throughput density functional theory (HT-DFT) (10) have resulted in massive computational databases of materials properties (11–15), containing the calculated properties of hundreds of thousands of experimentally reported and hypothetical materials. Such databases have led to new data-driven approaches toward understanding materials. Here we

introduce a novel paradigm of viewing materials, and equilibrium phase diagrams in particular, via the lens of complex network theory, i.e. studying the similarities and interactions between materials themselves, in striking contrast to the traditional bottom-up approaches toward unlocking structure-property relationships in materials (16, 17).

We use the Open Quantum Materials Database (OQMD) (11, 12), a HT-DFT database containing calculations of nearly all crystallographically ordered, structurally unique materials experimentally observed to date (as collected in the Inorganic Crystal Structure Database (18) repository) and a large number of hypothetical materials constructed using commonly occurring structural prototypes—a total of more than half a million materials—to extract the “universal phase stability network” or the “universal  $T=0$  K phase diagram”. We accomplish this by using all the phase data in the OQMD within a convex-hull formalism, and identifying *all* thermodynamically stable materials and *all* two-phase equilibria between them. We then represent stable materials as nodes and two-phase equilibria (tie-lines) as edges, thus describing a  $T=0$  K phase diagram as a network encoding thermodynamic stability (illustrated with schematics in Fig. 1).

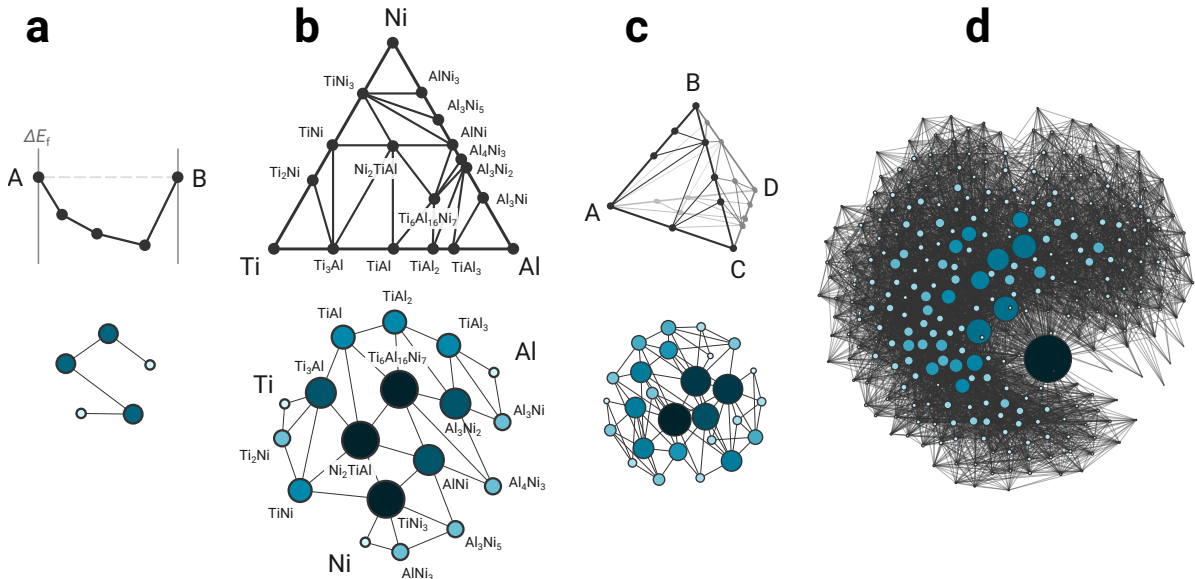


**Fig. 1. Network representation of  $T=0$  K materials phase diagrams.** Stable phases and two-phase equilibria (tie-lines) in a phase diagram are represented as nodes and edges, respectively, to create the corresponding network: (a) Schematic A-B binary system represented as a typical two-dimensional convex hull of compound formation energies. (b) Ti-Ni-Al as an example ternary system, with the  $T=0$  K phase diagram shown as a Gibbs triangle. (c) Schematic A-B-C-D quaternary phase diagram shown as a Gibbs tetrahedron. (d) The 3d transition metal-chalcogen (i.e. 14-dimensional chemical space) materials network. No conventional visual representations exist of phase diagrams at higher than 4 dimensions. Node sizes shown are proportional to node degree.

# Results

## Overall network connectivity

We find that the phase stability network of all inorganic materials consists of  $\sim 21,300$  nodes and is remarkably dense with a total of nearly 41 million edges, and extremely well-connected with  $\sim 3,850$  edges per node on average (“mean degree”  $\langle k \rangle$ ). This means that every stable inorganic compound can form a stable two-phase equilibrium with 3,850 other compounds on average. For comparison,  $\langle k \rangle$  for other widely-studied networks range from 1.4 (network of email messages) to 113.4 (collaboration network of film actors) (19). The connectance of the materials network, or the fraction of the maximum possible number of edges that are actually present is 0.18. This is an important statistic for the design of “systems of materials”, such as electrodes and electrolytes making up batteries (20), or coating materials separating two reactive components (21), where the longevity of the system relies on stable coexistence of such components. Using a lithium-ion intercalation battery as an example “system of materials”, a common approach to tackling electrode degradation is to apply protective coatings on electrode particles. In such a battery, the material in the electrode coating should not react with/be consumed by materials in the electrode *as well as* those in the electrolyte (22, 23). Thus, the coating–electrode and the coating–electrolyte material pairs must both have tie-lines with each other in order to stably coexist in the system. In other words, both pairs must be neighboring, connected nodes in the materials network.

The degree distribution in the complete phase stability network, specifically the probability  $p(k)$  that a material has a tie-line with  $k$  other materials in the network follows a lognormal form (Fig. 2a, and Fig. 1 in the Supplementary Materials). While many widely-studied networks are known to have scale-free power-law degree distributions, lognormal distributions are another member of the “heavy-tail” family, are also relatively common, and behave quite similar to power-laws (24). In fact, sparsity has been shown to be a necessary condition for the emergence of an exact power-law behavior (25), and densification in sparse, scale-free networks leads to distributions that deviate from a power-law and become closer to lognormal. Thus, the lognormal behavior of the materials network can be understood to result from its extremely dense connectivity, in contrast to the general sparsity of commonly-studied networks.

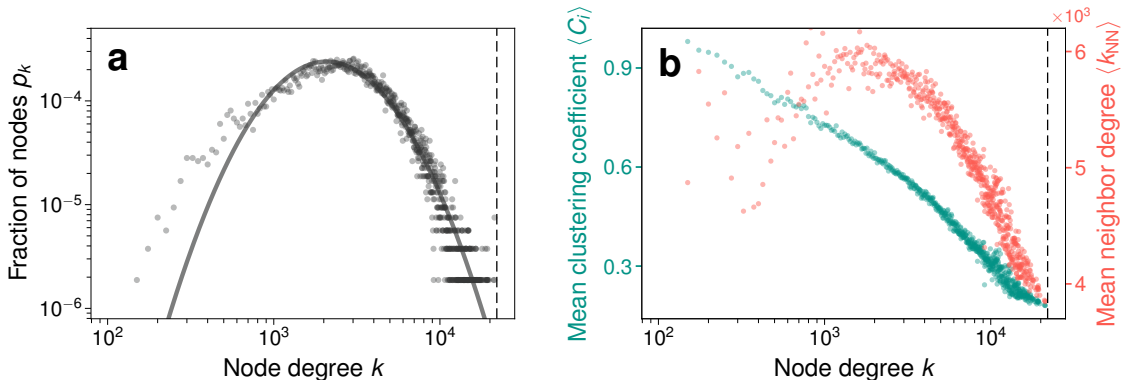


**Fig. 2. Overall structure and topology of the materials network.** (a) The distribution of node degree in the materials network (grey circles) shows a heavy tail, i.e. a sizeable fraction of materials have tie-lines with nearly all other materials. A lognormal fit is shown as a solid grey line. (b) The mean local clustering coefficient  $\langle C_i \rangle$  (green) decreases with node degree  $k$  indicating that stable materials form local, high-connected communities. The mean neighbor degree  $\langle k_{NN} \rangle$  (red) also decreases with  $k$ , implying a weakly-dissortative network behavior, i.e. materials with a large number of tie-lines connect with those with fewer tie-lines in the network. In both subplots, the vertical dashed line represents the total number of nodes (stable materials) in the network.

## Network topology

The characteristic path length or mean node-node distance in a network,  $\mathcal{L}$ , is defined as the number of edges in the shortest path between two nodes, averaged over all pairs of nodes. The longest node-node distance in the network defines its diameter,  $\mathcal{L}_{\max}$ . The characteristic path length of the materials network  $\mathcal{L} = 1.8$ , and its diameter  $\mathcal{L}_{\max} = 2$ . This remarkably short path length indicates that the materials network has “small-world” characteristics (1), i.e. despite its large size, the number of edges that need to be traversed from a given node to any other node is relatively small. The extremely small  $\mathcal{L}$  for the materials network can be intuitively understood to be a consequence of the almost complete lack of reactivity of noble gases. The non-participation of noble gases in the formation of compounds (and thus having tie-lines with nearly all materials in the network) places an upper bound of 2 on  $\mathcal{L}_{\max}$ , and since some material pairs already have tie-lines that connect them immediately, the mean path  $\mathcal{L}$  is slightly smaller than 2. Even if noble gases are disregarded, the mean path length and diameter of the materials network remain small due to the presence of a few other very-highly connected nodes corresponding to extremely stable and non-reactive materials, e.g. binary halides.

Another metric of interest in a real-world network is transitivity or clustering, quantified by its clustering coefficient,  $\mathcal{C}$ , which is the probability that two nodes connected to the same third node

are themselves connected. In other words, given that there exist stable two-phase equilibria A–C and B–C, what is the probability that A and B can stably coexist? Depending on how the averaging is performed, a global ( $\mathcal{C}_g$ ) or mean local ( $\bar{\mathcal{C}}_i$ ) cluster coefficient of a network can be defined (1, 19). For the materials network, the clustering coefficients are  $\mathcal{C}_g = 0.41$  and  $\bar{\mathcal{C}}_i = 0.55$ , comparable to other real-world networks, and much higher than random networks of the same density. The mean local clustering coefficient of the materials network decreases with increasing node connectivity (Fig. 2b), indicating that stable materials form local highly-connected communities in the network, and such behavior often suggests a hierarchical network structure (26). The assortativity coefficient or the Pearson correlation coefficient of degree between pairs of connected nodes in the materials network is  $-0.13$ , indicating weakly dissortative mixing behavior. This is also confirmed by the distribution of the mean degree of neighbors of a node of degree  $k$  being a decreasing function of  $k$  (Fig. 2a). In other words, materials with a high  $k$  (i.e. large number of tie-lines) tend to connect with materials with a lower  $k$  (i.e. smaller number of tie-lines). This weakly dissortative behavior of the materials network is similar to that observed in most other technological, information, biological networks, and is likely a virtue of such networks being simple graphs (27).

### Hierarchy in the materials network

The mean degree or the average number of tie-lines per material  $\langle k \rangle$  decreases with the number of components,  $\mathcal{N}$  ( $\mathcal{N} = 2$  for binary,  $\mathcal{N} = 3$  for ternary, etc. See Fig. 3a), indicating a chemical hierarchy in the materials network. This can be understood to result from an inherent competition for tie-lines that high- $\mathcal{N}$  materials face with low- $\mathcal{N}$  materials in their chemical space, but not vice-versa. In other words, ternary compounds  $X_aY_bZ_c$  compete not only with other compounds in the  $X$ - $Y$ - $Z$  chemical space but also with binary compounds in the  $X$ - $Y$ ,  $Y$ - $Z$ ,  $Z$ - $X$  spaces for tie-lines.

We note that this decrease in  $\langle k \rangle$  with  $\mathcal{N}$  is distinct from the distribution of number of stable  $\mathcal{N}$ -ary materials itself (Fig. 3a), which shows a peak at  $\mathcal{N} = 3$ . Does this peak in the distribution of stable materials imply the existence of infinite, underexplored space for the discovery of new materials beyond ternaries? The distribution of formation energies of materials as a function of number of components  $\mathcal{N}$  (Fig. 3b) reflects the consequence of competition between low- and high-component materials: high- $\mathcal{N}$  compounds appear to need significantly lower formation energies than low- $\mathcal{N}$  ones to become stable. Since there is no obvious underlying reason for the distribution

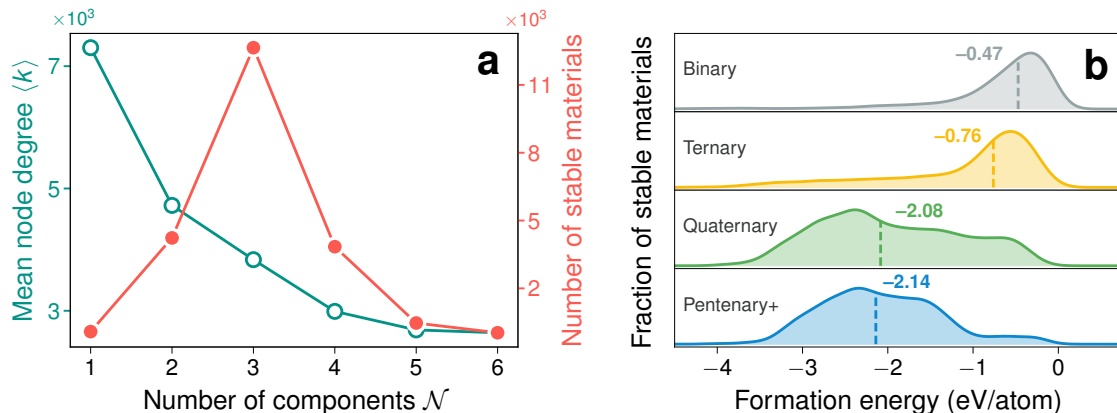


**Fig. 3. Hierarchy in the materials network, and underlying energetic considerations.** (a) The mean node degree or average number of tie-lines  $\langle k \rangle$  (green, open) decreases as a function of number of components  $\mathcal{N}$  (i.e. binary, ternary, and so on), which results from high- $\mathcal{N}$  materials having to compete with low- $\mathcal{N}$  materials for stability. The number of known stable  $\mathcal{N}$ -ary materials (red) itself actually peaks at  $\mathcal{N} = 3$  (ternaries). (b) Gaussian kernel density estimates of compound formation energies for all stable materials separated by number of components in the material. Dotted vertical lines indicate the respective median of each distribution. High- $\mathcal{N}$  need significantly lower formation energies than low- $\mathcal{N}$  materials to become stable, e.g.  $-2.08$  versus  $-0.47$  eV/atom for quaternary and binary materials, respectively.

of  $T = 0$  K formation energies (with entropic effects neglected) to differ significantly with  $\mathcal{N}$ , only a few high- $\mathcal{N}$  materials can “survive” as stable phases if the corresponding lower- $\mathcal{N}$  systems already have several stable phases. This is consistent with the recent reports of a “volcano plot” that emerges for stable inorganic ternary nitrides as a function of energetic competition with their corresponding binary nitrides (28), and an increased probability of phase separation with increasing number of components in a material system (29). Widom (30) further argued that the a peak near  $\mathcal{N} = 3$  or 4 in such distributions arises from a competition between combinatorial explosion and diminishing volume-to-surface ratio in the composition simplex, as  $\mathcal{N}$  increases. Thus, although we do not know of a fundamental law limiting access to thermodynamically stable materials with higher components, a combination of the hierarchy observed in the phase stability network, the distribution of formation energies, and the topology of the convex energy surface all suggest that the scarcity of known high- $\mathcal{N}$  stable materials is not merely a consequence of those chemical spaces being underexplored.

### Knowledge extraction: material nobility index

Since the phase stability network practically encompasses all known inorganic crystalline materials as well as a large number of predicted hypothetical materials, the number of tie-lines emerges as

a natural metric of nobility of a crystalline material—it is simply the count of other materials it is determined to have no reactivity against. Thus, while material reactivity or nobility have no standard definitions, a network representation of materials enables us to tackle the chemical nobility of inorganic materials in solid-solid and solid-gas reactions in a completely data-driven fashion, instead of the traditional intuitive or heuristic approaches. Since the number of tie-lines in the materials network is lognormally distributed, we devise a new standard score of material nobility, the “nobility index”:

$$\mathcal{Z}_n = \frac{\ln(k) - \mu}{\sigma} \quad (1)$$

where  $k$  is the node degree or the number of tie-lines a material has, and  $\mu = 8.06$  and  $\sigma = 0.65$  are the mean and standard deviation of the underlying lognormal distribution. The nobility index is thus agnostic of textbook classifications such as metal, nonmetal, metalloid, ionic, covalent, and so on, and works equally well for any given material. Since the tie-lines in the network are as computed with DFT, the nobilities of materials predicted herewith are only limited by DFT accuracy in estimating relative stabilities of inorganic materials (12, 29, 31).

First, we tackle the reactivity or nobility of elements. Noble gases and fluorine form the bounds of the nobility index (Fig. 4), as the noblest and the most reactive, respectively, not only among the elements but in fact among all materials in the network. The most reactive elements following F are P, S, and Cl. Alkali and alkaline earth metals, often considered to be highly reactive metals, are relatively noble in solid-solid and solid-gas reactions, in comparison to early  $d$ -block or lanthanide elements, which are, along with Al, the most reactive metals. The nobility index increases down a group for metals, and increases (decreases) from left-to-right along a row of the periodic table within the  $d$ -block ( $s$ -block). But what is the noblest metal of them all? Ag emerges as the noblest of all elements after noble gases, followed closely by Hg, Os, Re, W, and Cu, all having more than 14,000 tie-lines. Gold, traditionally considered the noblest element (32), despite being relatively densely connected with 10,000 tie-lines, is less noble in solid-state reactions. Finally, we find that  $\mathcal{Z}_n$  is not correlated with other common elemental properties such as electronegativity, atomic radii, melting point, and others (33), indicating that the nobility index encodes new information not readily captured by those properties (Fig. 2 in the Supplementary Materials).

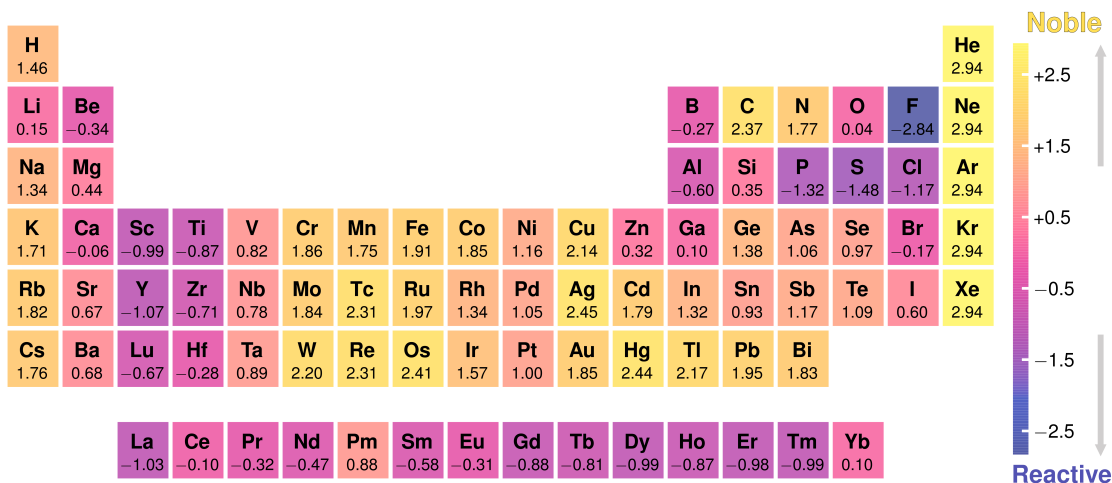


**Fig. 4. Nobility index of all elements.** The standard score,  $\mathcal{Z}_n$ , derived in this work using material connectivity in the phase stability network, as a measure of nobility against solid-solid and solid-gas reactions. Nobility increases up the scale. Numerical values of elemental  $\mathcal{Z}_n$  are given below the respective symbols.

Beyond elements, what are the noblest inorganic compounds of all? The compounds at the top of the nobility list are IA/IIA-VIIA compounds such as LiF, NaCl, KCl, CsCl, KBr, CsBr, KI, RbI, CaF<sub>2</sub>, SrF<sub>2</sub>, CsYbF<sub>3</sub>, RbYbF<sub>3</sub>, and others, their inertness likely due to stability from strong ionic bonding between their constituents. We exclude rareearth- and actinide-containing compounds from the previous analysis of compound nobility in order to account for any shortcomings in the DFT description of *f*-block elements and compounds containing them.

## Discussion

While some of our findings above are in line with chemical intuition, relative nobilities in certain cases, e.g. silver vs gold, deviate from it. This deviation is in part due to the historical context in which these materials have been considered noble or reactive, e.g. whether an element oxidizes or corrodes readily in air, reacts with water and/or certain acids, dissolves in water or electrolytes, and how vigorous such reactions seem. More fundamental approaches to finding descriptors for reactivity go back to electronegativity related concepts, followed by interrelated theories based on perturbation theory, derivatives of electronic energy such as hardness and softness, and others largely developed for molecules (34–36). In contrast, the nobility index,  $\mathcal{Z}_n$ , as derived from the tie-lines in the network of all inorganic materials represents a general metric emerging directly from bulk thermodynamic data.

High-throughput experimental and computational techniques are leading to an explosive growth in the size of materials databases. Representation and interpretation of the data at a large-scale, however, remains a challenge. Here we show that tools from complex network theory enable us to access otherwise-difficult-to-extract information from such large datasets. In other words, the emergence of material reactivity from the collective behavior of all materials in the phase stability network serves as a simple, preliminary example of knowledge extraction out of complex networks of materials. Other similar approaches can be used to discover other hidden knowledge, e.g. analysis of “communities” or “cliques” in the network of all materials can uncover hitherto-unknown relationships between various known materials.

Further, there are various ways our graph theoretic approach to materials data can be used to immediately applied to new materials discovery and design: (a) *direct* techniques, e.g. metrics from network theory such as local clustering and similarity can be used to identify “holes” in the current network—where nodes (i.e. materials) are expected to exist but currently do not, and (b) *indirect* techniques, e.g. using the extracted knowledge or quantities derived from the network as input to other approaches such as in materials informatics. For example, using temporal materials discovery information in combination with thermodynamic phase stability networks can help predict synthesizability (37). Furthermore, while some of its features resemble other complex networks, the extremely-high connectance and the lognormal degree distribution of the presented phase stability network imply that its underlying generative mechanisms may be unique, and developing generative models for such materials networks can have significant impact on the knowledge discovery of materials in the future.

## Methods

All convex hull constructions were performed using the *Qhull* library (38) as implemented in the *qmpy* ([pypi.org/project/qmpy](https://pypi.org/project/qmpy)) package. All network analyses were performed using the *graph-tool* (39) and *powerlaw* (40) packages, and comparison of heavy-tailed distributions is done according to the method of log likelihood ratios as described in Clauset et al. (41). Details of the divide-and-conquer approach used to tackle the combinatorial explosion in calculating the universal phase diagram, the related exponential increase in the time complexity to construct convex hulls in higher dimen-

sions (42), its network representation, and determining the node degree distribution are provided in the Supplementary Materials.

## References

- [1] D. J. Watts, S. H. Strogatz, Collective dynamics of ‘small-world’ networks. *Nature* **393**, 440–442 (1998).
- [2] R. Albert, H. Jeong, A.-L. Barabási, Diameter of the world-wide web. *Nature* **401**, 130 (1999).
- [3] D. J. Watts, P. S. Dodds, M. E. Newman, Identity and search in social networks. *Science* **296**, 1302–1305 (2002).
- [4] M. E. J. Newman, The structure of scientific collaboration networks. *Proc. Natl. Acad. Sci. USA* **98**, 404–409 (2001).
- [5] R. J. Williams, N. D. Martinez, Simple rules yield complex food webs. *Nature* **404**, 180 (2000).
- [6] R. Guimerà, L. A. Nunes Amaral, Functional cartography of complex metabolic networks. *Nature* **433**, 895–900 (2005).
- [7] A.-L. Barabási, R. Albert, Emergence of scaling in random networks. *Science* **286**, 509–512 (1999).
- [8] S. H. Strogatz, Exploring complex networks. *Nature* **410**, 268 (2001).
- [9] H. Jeong, R. Tombor, R. Albert, Z. N. Oltvai, A.-L. Barabási, The large-scale organization of metabolic networks. *Nature* **407**, 651–654 (2000).
- [10] S. Curtarolo, G. L. W. Hart, M. B. Nardelli, N. Mingo, S. Sanvito, O. Levy, The high-throughput highway to computational materials design. *Nat. Mater.* **12**, 191–201 (2013).
- [11] J. E. Saal, S. Kirklin, M. Aykol, B. Meredig, C. Wolverton, Materials design and discovery with high-throughput density functional theory: the Open Quantum Materials Database (OQMD). *JOM* **65**, 1501 (2013).
- [12] S. Kirklin, J. E. Saal, B. Meredig, A. Thompson, J. W. Doak, M. Aykol, S. Rühl, C. Wolverton, The Open Quantum Materials Database (OQMD): assessing the accuracy of DFT formation energies. *npj Comput. Mater.* **1**, 15010 (2015).
- [13] A. Jain, S. P. Ong, G. Hautier, W. Chen, W. D. Richards, S. Dacek, S. Cholia, D. Gunter, D. Skinner, G. Ceder, K. Persson, The Materials Project: A materials genome approach to accelerating materials innovation. *APL Mater.* **1**, 011002 (2013).
- [14] S. Curtarolo, W. Setyawan, S. Wang, J. Xue, K. Yang, R. H. Taylor, L. J. Nelson, G. L. W. Hart, S. Sanvito, M. Buongiorno-Nardelli, N. Mingo, O. Levy, aflowlib.org: a distributed materials properties repository from high-throughput ab initio calculations. *Comput. Mater. Sci.* **58**, 227 (2012).

- [15] J. Hachmann, R. Olivares-Amaya, S. Atahan-Evrenk, C. Amador-Bedolla, R. S. Sánchez-Carrera, A. Gold-Parker, L. Vogt, A. M. Brockway, A. Aspuru-Guzik, The Harvard clean energy project: Large-scale computational screening and design of organic photovoltaics on the world community grid. *J. Phys. Chem. Lett.* **2**, 2241–2251 (2011).
- [16] M. T. Dove, *Structure and dynamics: an atomic view of materials* (Oxford University Press, 2003).
- [17] R. Phillips, *Crystals, Defects and Microstructures: Modeling Across Scales* (Cambridge University Press, 2001).
- [18] A. Belsky, M. Hellenbrandt, V. L. Karen, P. Luksch, New developments in the Inorganic Crystal Structure Database (ICSD): accessibility in support of materials research and design. *Acta Cryst. B* **58**, 364–369 (2002).
- [19] M. E. J. Newman, The Structure and Function of Complex Networks. *SIAM Review* **45**, 167–256 (2003).
- [20] S. P. Ong, Y. Mo, W. D. Richards, L. Miara, H. S. Lee, G. Ceder, Phase stability, electrochemical stability and ionic conductivity of the  $\text{Li}_{10\pm 1}\text{MP}_2\text{X}_{12}$  ( $\text{M} = \text{Ge}, \text{Si}, \text{Sn}, \text{Al}$  or  $\text{P}$ , and  $\text{X} = \text{O}, \text{S}$  or  $\text{Se}$ ) family of superionic conductors. *Energy Environ. Sci.* **6**, 148–156 (2013).
- [21] M. Aykol, S. Kim, V. I. Hegde, D. Snyder, Z. Lu, S. Hao, S. Kirklin, D. Morgan, C. Wolverton, High-throughput computational design of cathode coatings for Li-ion batteries. *Nat. Commun.* **7**, 13779 (2016).
- [22] M. Aykol, S. Kim, V. I. Hegde, D. Snyder, Z. Lu, S. Hao, S. Kirklin, D. Morgan, C. Wolverton, High-throughput computational design of cathode coatings for Li-ion batteries. *Nat. Commun.* **7**, 13779 (2016).
- [23] D. H. Snyder, V. I. Hegde, C. Wolverton, Electrochemically Stable Coating Materials for Li, Na, and Mg Metal Anodes in Durable High Energy Batteries. *J. Electrochem. Soc.* **164**, A3582–A3589 (2017).
- [24] M. Mitzenmacher, A brief history of generative models for power law and lognormal distributions. *Internet Math.* **1**, 226–251 (2003).
- [25] C. I. Del Genio, T. Gross, K. E. Bassler, All Scale-Free Networks Are Sparse. *Phys. Rev. Lett.* **107**, 178701 (2011).
- [26] E. Ravasz, A.-L. Barabási, Hierarchical organization in complex networks. *Phys. Rev. E* **67**, 026112 (2003).
- [27] S. Maslov, K. Sneppen, A. Zaliznyak, Detection of topological patterns in complex networks: correlation profile of the internet. *Physica A* **333**, 529–540 (2004).
- [28] W. Sun, C. J. Bartel, E. Arca, S. R. Bauers, B. Matthews, B. Orvañanos, B.-R. Chen, M. F. Toney, L. T. Schelhas, W. Tumas, J. Tate, A. Zakutayev, S. Lany, A. M. Holder, G. Ceder, A map of the inorganic ternary metal nitrides. *Nat. Mater.* **18**, 732–739 (2019).
- [29] W. Sun, S. T. Dacek, S. P. Ong, G. Hautier, A. Jain, W. D. Richards, A. C. Gamst, K. A. Persson, G. Ceder, The thermodynamic scale of inorganic crystalline metastability. *Sci. Adv.* **2**, e1600225 (2016).

- [30] M. Widom, Frequency Estimate for Multicomponent Crystalline Compounds. *J. Stat. Phys.* **167**, 726–734 (2017).
- [31] M. Aykol, S. S. Dwaraknath, W. Sun, K. A. Persson, Thermodynamic limit for synthesis of metastable inorganic materials. *Sci. Adv.* **4**, eaaq0148 (2018).
- [32] B. Hammer, J. K. Norskov, Why gold is the noblest of all the metals. *Nature* **376**, 238–240 (1995).
- [33] L. Ward, A. Agrawal, A. Choudhary, C. Wolverton, A general-purpose machine learning framework for predicting properties of inorganic materials. *npj Comput. Mater.* **2**, 16028 (2016).
- [34] G. Klopman, Chemical Reactivity and the Concept of Charge- and Frontier-Controlled Reactions. *J. Am. Chem. Soc.* **90**, 223–234 (1968).
- [35] W. Yang, R. G. Parr, Hardness, softness, and the Fukui function in the electronic theory of metals and catalysis. *Proc. Natl. Acad. Sci. USA* **82**, 6723–6726 (1985).
- [36] H. Chermette, Chemical reactivity indexes in density functional theory. *J. Comput. Chem.* **20**, 129–154 (1999).
- [37] M. Aykol, V. I. Hegde, L. Hung, S. Suram, P. Herring, C. Wolverton, J. S. Hummelshøj, Network analysis of synthesizable materials discovery. *Nat. Commun.* **10**, 2018 (2019).
- [38] C. B. Barber, D. P. Dobkin, H. Huhdanpaa, The quickhull algorithm for convex hulls. *ACM Trans. Math. Softw.* **22**, 469–483 (1996).
- [39] T. P. Peixoto, The graph-tool python library. *figshare* (2014).
- [40] J. Alstott, E. Bullmore, D. Plenz, Powerlaw: a Python package for analysis of heavy-tailed distributions. *PLoS ONE* **9**, e85777 (2014).
- [41] A. Clauset, C. R. Shalizi, M. E. J. Newman, Power-Law Distributions in Empirical data. *SIAM Rev.* **51**, 661–703 (2009).
- [42] H. Sartipizadeh, T. L. Vincent, Computing the Approximate Convex Hull in High Dimensions. Preprint at <https://arxiv.org/abs/1603.04422> (2016).

## Acknowledgements

**Funding:** V.I.H. acknowledges support from Toyota Research Institute (TRI) through the Accelerated Materials Design and Discovery program. C.W. acknowledges the support of the National Science Foundation (NSF), through the MRSEC program, grant number DMR-1720139. **Author contributions:** V.I.H. and M.A. conceived and designed the project, and contributed equally to this work. M.A. calculated all the tie-lines in the materials network. V.I.H. performed the network analysis and nobility index calculations. S.K. wrote the code to calculate convex hulls. C.W.

supervised the project. All authors contributed toward writing the manuscript. **Competing interests:** None. **Data availability:** All data needed to evaluate the conclusions in the paper are present in the paper, the Supplementary Materials, or is available to download at no cost from the OQMD website (<http://oqmd.org>). Additional data related to this paper may be requested from the authors.

## Supplementary Materials

Supplementary Text (divide-and-conquer calculation of the universal phase diagram, fitting degree distributions, and novel materials knowledge captured by the nobility index)

Figs. S1–S3

Table S1 with compute times for determining tie-lines

References

# Supplementary Materials

## The Phase Stability Network of All Inorganic Materials

Vinay I. Hegde,<sup>1,\*</sup> Muratahan Aykol,<sup>2,\*‡</sup> Scott Kirklin,<sup>1,†</sup> and Chris Wolverton<sup>1,‡</sup>

<sup>1</sup>*Department of Materials Science and Engineering,  
Northwestern University, Evanston, IL 60208*

<sup>2</sup>*Toyota Research Institute, Los Altos, CA 94022*

---

\*These authors contributed equally to this work

†Current address: Jump Trading LLC, Chicago, IL 60654

‡Email: [c-wolverton@northwestern.edu](mailto:c-wolverton@northwestern.edu) (C. Wolverton), [murat.aykol@global.tri](mailto:murat.aykol@global.tri) (M. Aykol)

We describe the approach used to calculate the universal phase diagram, its network representation and determining the node degree distribution in the network in the following sections S1–S2.

## S1. Calculation of the $T = 0$ K universal phase diagram

The  $T = 0$  K phase diagram for a given chemical space is determined by the so-called convex hull construction. A phase is thermodynamically stable iff it lies on (i.e. is a vertex of) the convex hull of  $T = 0$  K formation energies of all phases in the chemical space. And phases that are directly connected by a tie-line, i.e., phases that lie on the same facet of the convex hull, are in equilibrium with one another. Determining a binary A-B phase diagram requires constructing a 2-dimensional convex hull of formation energies of all  $A_xB_y$  compounds (composition  $x$  and formation energy being the two dimensions), a ternary A-B-C phase diagram requires constructing a 3-dimensional convex hull of formation energies of all  $A_xB_yC_z$  compounds (compositions  $x$  and  $y$ , and formation energy being the three dimensions), and so on. The determination of an  $d$ -nary phase diagram requires the construction of an  $d$ -dimensional convex hull of formation energies of all the  $N$  phases in the chemical space.

For low dimensions, i.e.  $d = 2$  or  $3$  (binary or ternary systems), finding the convex hull of  $N$  points (total number of phases) has a worst-case time complexity of  $\mathcal{O}(N \log N)$ . For higher dimensions, standard methods of determining convex hulls such as the Quickhull algorithm, have worst-case time complexities of  $\mathcal{O}(N^{[d/2]})$  (1). For random data, even the average-case time complexity at higher dimensions scales as  $\mathcal{O}(\log^{d-1} N)$ , i.e. exponentially with  $d$  (2). Such scaling behaviors mean that for moderately large number of points  $N$  and dimensions  $d$ , finding the convex hull becomes increasingly practically challenging. For instance, to find the convex hull of all known inorganic materials, even restricting ourselves to experimentally reported compounds in the Open Quantum Materials Database (OQMD),  $N \approx 40,000$  and  $d = 89$ , making the calculation of the convex hull practically impossible with a traditional single-shot approach.

We tackle this challenge of calculating the convex hull at high-dimensions by using a divide-and-conquer approach. While the representational complexity of the convex-hull increases at least exponentially with  $d$ , we know from the set of existing materials that not many of them are high-dimensional by themselves. In fact, 99.5% of materials in the OQMD have 4 unique elemental components or fewer. Since the stability of a material is determined only within the chemical

Phase 1	Phase 2	# Components	Time (s)
Na <sub>2</sub> O	KCl	4	~3
Fe <sub>2</sub> S <sub>3</sub>	Li <sub>2</sub> MnO <sub>4</sub>	5	~6
Li <sub>3</sub> PS <sub>4</sub>	SrTiO <sub>3</sub>	6	~8
Ba <sub>2</sub> Li <sub>3</sub> TaN <sub>4</sub>	LiCoO <sub>2</sub>	6	~14
Ba <sub>2</sub> Li <sub>3</sub> TaN <sub>4</sub>	NaCoO <sub>2</sub>	7	~32
Mn <sub>2</sub> Hg <sub>2</sub> SF <sub>6</sub>	Li <sub>4</sub> CrCoO <sub>6</sub>	8	~34
Mn <sub>2</sub> Hg <sub>2</sub> SF <sub>6</sub>	Ba <sub>2</sub> Ca <sub>3</sub> Tl <sub>2</sub> Cu <sub>4</sub> O <sub>12</sub>	9	~65

**Table 1. Sample compute times for calculating the existence of a tie-line between two phases.** The time required is highly dependent on the number of components, i.e. unique elements in the combined chemical space, and further depends on the number of all known compounds in the chemical space. Each calculation was performed on a standard desktop computer utilizing a single core.

subspace of elements that it is made of, we first determine the vertices (i.e. stable materials) of the 89-dimensional convex hull at a reduced computational cost by computing the convex hulls in low-dimensional subspaces for each individual material separately. For instance, to determine if the compound CaMnO<sub>3</sub> is stable, it is sufficient to construct the convex hull of all phases Ca<sub>x</sub>Mn<sub>y</sub>O<sub>z</sub> in the Ca-Mn-O subspace. This process of constructing convex hulls separately for each unique chemical subspace yields all the vertices of the full convex hull:  $\sim 2.1 \times 10^4$  stable materials out of the  $> 5.5 \times 10^5$  total materials calculated in the OQMD. Having determined the vertices of the full convex hull, in the second stage, we exhaustively evaluate the existence of a tie-line between any given pair of stable compounds in the OQMD by constructing the convex hull of formation energies in the combined chemical spaces of such candidate pairs, rather than the full 89-dimensional space itself. For example, to determine whether there exists a tie-line between Li<sub>2</sub>O and NaCl, we construct the Li-Na-Cl-O convex hull, and find that there indeed exists a Li<sub>2</sub>O-NaCl tie-line. In contrast, from a Na-K-F-Cl convex hull we find that NaCl and KF, in fact, “react” to form a NaF-KCl two-phase equilibrium. Overall, we construct convex hulls for all  $^{2.1 \times 10^4}C_2 \approx 2.3 \times 10^8$  stable phase combinations, and find a total  $\sim 41 \times 10^6$  tie-lines.

The computational cost of constructing a convex hull for a unique chemical subspace is expectedly highly dependent on the number of components, and ranges from a few seconds to a few minutes on a standard desktop computer utilizing a single core (some sample times for checking if a tie-line exists between two known materials are provide in Table 1). With a conservative estimate of 15–20 seconds per tie-line, the total time required to exhaustively evaluate all possible tie-lines is more than 1 million CPU hours.

We then represent stable compounds as nodes and tie-lines as edges, thereby generating the “universal phase diagram” as a complete thermodynamic phase stability network of all inorganic materials. We use the *Qhull* library (1) as implemented in the *qmpy* package ([pypi.org/project/qmpy](http://pypi.org/project/qmpy)) for all the convex hull calculations reported in this work.

## S2. Degree distribution of the network of all materials

The probability distribution of node connectivity (number of tie-lines a material has) in the phase stability network of all inorganic materials is heavy-tailed. We examine which of the common heavy-tailed distributions best fit our empirical data. In particular, several well-studied technological, social, and biological networks are thought to have power-law distributions. Is the thermodynamic network of materials similar to other common natural/man-made networks exhibiting power-law behavior or not? To answer this question, we directly compare pairs of heavy-tailed distributions using the method of log likelihood ratios as described in Clauset et al. (3). For the full materials network, we find that a lognormal distribution ( $\mu = 8.06$ ,  $\sigma = 0.65$ ) is the best fit by far (see Fig. 1).

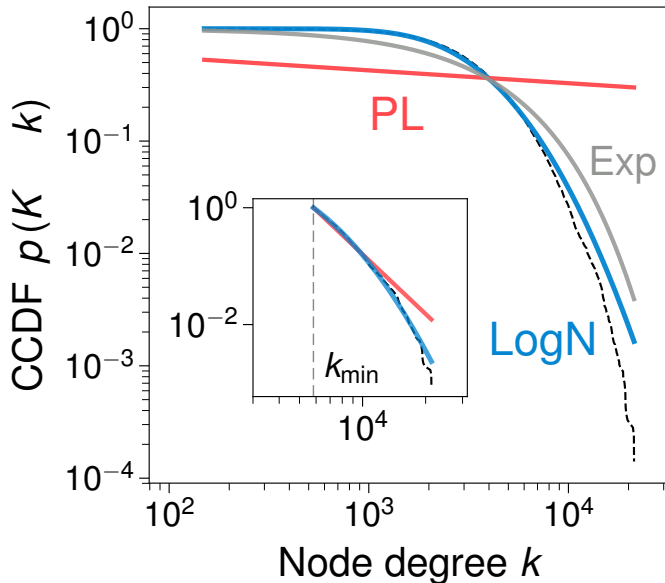


**Fig. 1. Fitting node connectivity data to candidate distributions.** The complementary cumulative distribution function of the node degree in the network of all materials is shown as dashed black lines. Power-law (PL), lognormal (LogN), and exponential (Exp) distributions fit to the data are shown as solid red, blue, and grey lines, respectively. The inset shows power-law and lognormal fits to the *tail* of the degree distribution for degree  $k > k_{\min} = 5800$ .

We note that most empirical phenomena obey power-laws only for values greater than some

minimum value, i.e. only the tail of the distribution follows a power-law. We investigate if this is indeed the case for the materials network. We find the optimal lower-bound for a power-law behavior,  $k_{\min}$ , for the materials network as the value that minimizes the Kolmogorov-Smirnov distance between the data and the fit (3). We find  $k_{\min}$  for the materials network =  $\sim 5800$ , and the power-law scaling parameter  $\alpha = 4.4$ . We note that a  $k_{\min}$  of 5800 retains only 17% of the overall materials network (i.e. only 17% of all materials have more than 5800 tie-lines each). Furthermore, even over this tail region of the degree distribution, a lognormal distribution is a better fit (see the inset in Fig. 1): the log likelihood ratio  $\mathcal{R}$  for power-law versus lognormal is  $-7.15$  with a  $p$ -value of 0. In other words, even in the  $k_{\min} = 5800$  region (tail) of the materials network, the lognormal distribution fits the data far better than a power-law.

All analyses of fits of degree distributions mentioned above were performed with the *powerlaw* package (4). We note that the graph-theoretic analyses reported in this work (e.g. local clustering and centrality measures) performed with the *graph-tool* package (5), while requiring more than 8 G of memory, take a few hours on a standard desktop utilizing up to 4 cores.

### S3. New information encoded in the “nobility index”

A comparison of the nobility index  $\mathcal{Z}_n$  of elements against elemental properties such as electronegativity, boiling point, melting point, atomic volume, etc., as collected by Ward et al. (6) shows little correlation between  $\mathcal{Z}_n$  and other properties, with Pearson correlation coefficients close to 0 for most properties (see Fig. 2 for a sample comparison set). This indicates that the nobility index defined in this work truly encodes new information about an element/a material not adequately captured by other common properties.

Further, data-driven metrics such as nobility index capture materials knowledge that is not immediately intuitable or is sometimes even counter-intuitive. For instance, intuition derived only from a few elements and some of their compounds may imply that multivalent elements (e.g. transition metals) are likely to have a higher number of tie-lines than monovalent elements (e.g. alkali metals) simply by the virtue of a higher number of compound-forming possibilities. However, data from all materials known so far shows no correlation between number of compounds formed by an element and its total number of tie-lines (i.e. nobility; see Fig. 3). In fact, monovalent metals seem to form more compounds on average than their multivalent counterparts!

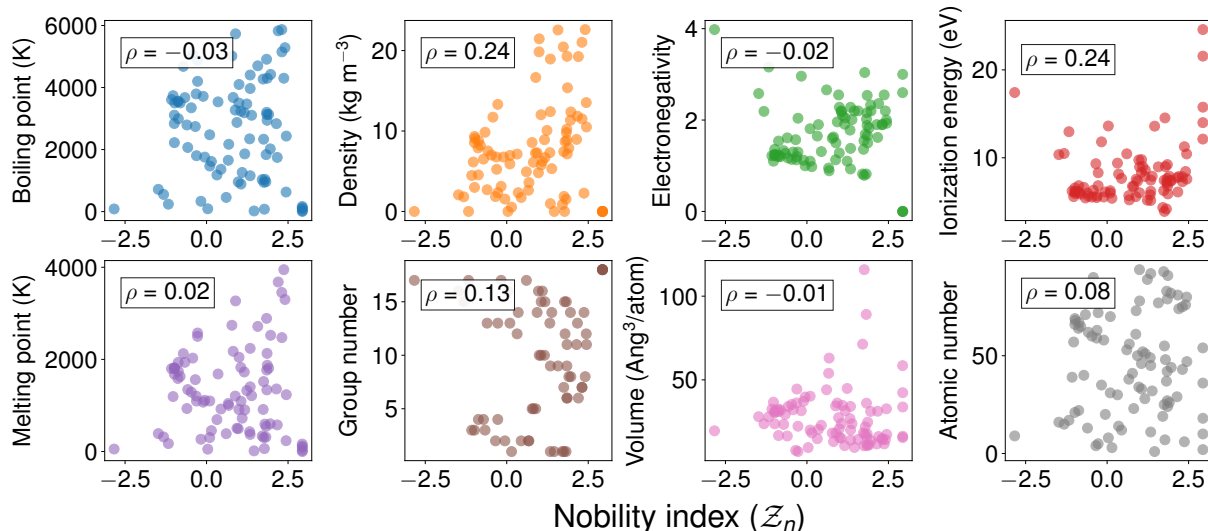


**Fig. 2. Comparison of nobility index versus common elemental properties.** There is little to no correlation between the nobility index of an element and any of its properties such as (counterclock-wise from top-left) boiling point, density, electronegativity, first ionization energy, atomic number, atomic volume, group in the periodic table, and melting point. The Pearson correlation coefficient  $\rho$  for each comparison is on the top-left of the corresponding panel.

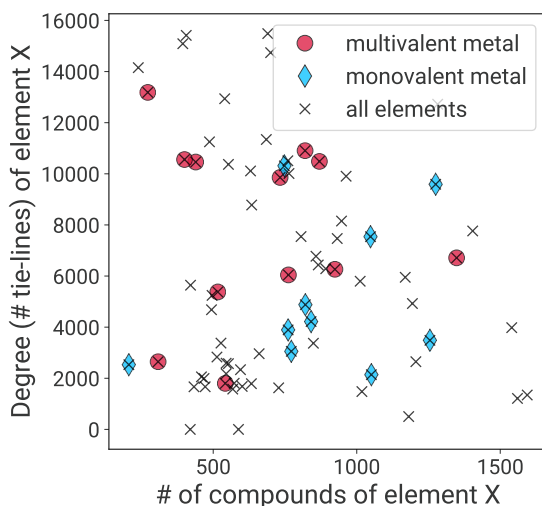


**Fig. 3. Comparison of number of compounds formed by an element versus its node degree.** Multivalent metals indicated are all transition metals (Ti, V, Cr, Mn, Fe, Co, Ni, Mo, W, Hf, Pd, Pt), and monovalent metals indicated are mostly alkali/alkaline earth metals (Li, Na, K, Rb, Be, Mg, Ca, Sr, Al, Zn).

## References

- [1] C. B. Barber, D. P. Dobkin, H. Huhdanpaa, The quickhull algorithm for convex hulls. *ACM Trans. Math. Softw.* **22**, 469–483 (1996).
- [2] H. Sartipizadeh, T. L. Vincent, Computing the Approximate Convex Hull in High Dimensions. Preprint at <https://arxiv.org/abs/1603.04422> (2016).
- [3] A. Clauset, C. R. Shalizi, M. E. J. Newman, Power-Law Distributions in Empirical data. *SIAM Rev.* **51**, 661–703 (2009).
- [4] J. Alstott, E. Bullmore, D. Plenz, Powerlaw: a Python package for analysis of heavy-tailed distributions. *PLoS ONE* **9**, e85777 (2014).
- [5] T. P. Peixoto, The graph-tool python library. *figshare* (2014).
- [6] L. Ward, A. Agrawal, A. Choudhary, C. Wolverton, A general-purpose machine learning framework for predicting properties of inorganic materials. *npj Comput. Mater.* **2**, 16028 (2016).